RSC Advances

PAPER

View Article Online
View Journal | View Issue

Cite this: *RSC Adv.*, 2024, **14**, 36656

Simple preparation of PVDF composite flexible film with transparent, self-cleaning and radiative cooling properties†

Junxia Mao, [a] Xinyu Tan,*[a] Weiwei Hu,[b] Chao Shi,[b] Fan Zhou[c] and Alkiviadis Tsamis[de]

Daytime radiative cooling is a technique that relies on reflecting sunlight and radiating heat through mid-infrared wavelengths to cool objects. However, most daytime radiative cooling materials are not transparent, cannot be used for vehicle windows or other objects that need to retain their original color, and are susceptible to rain, dust, and other contamination, resulting in reduced cooling performance. Here, we developed a transparent, self-cleaning, radiative cooling, highly flexible PVDF composite film (PPF film), which was prepared by solvent evaporation phase conversion method and scraping coating method. The preparation method is simple and the material is easy to obtain. The obtained PPF film can be crimped to different degrees, has high flexibility, a transmittance of 94% in the visible light range (380–760 nm), and a water contact angle of 105° and above, and has self-cleaning performance. In the range of 8–13 μm, the average emissivity of the film reached 94.42%. Outdoor experiments show that, on sunny days, the cavity temperature of the device coated with PPF film glass decreases by 5–6 °C compared with that of bare glass, indicating that the PPF film has excellent radiative cooling performance. In addition, it has relatively strong mechanical properties, ultraviolet aging resistance and acid and alkali resistance. The design of the PPF film enables the radiative cooling material to be transparent, self-cleaning and flexible, with broad application prospects in the outer surface of objects requiring light transmission and cooling, such as special-shaped curved surfaces, solar panels, and architectural glass.

Received 21st September 2024
Accepted 8th November 2024

DOI: 10.1039/d4ra06819j

rsc.li/rsc-advances

1. Introduction

For products that need to be used outdoors for a long time, such as solar cells and smart windows, high operating temperatures will adversely affect the application of the equipment after a long period of sunlight exposure. Therefore, reducing its surface temperature is a key way to solve this problem. Traditional cooling systems exacerbate global environmental problems by using large amounts of fossil energy to generate cooling electricity demand. As a technology that can realize passive cooling without additional energy, daytime radiant cooling systems have attracted wide attention for their great influence on energy-saving equipment[1–6] and have been widely used in various scenarios.[7–10] The radiative cooling material utilizes an atmospheric transparent window (8–13 μm) to emit heat into cold outer space, while also reflecting sunlight to prevent solar heating.[11–13] The ideal radiative cooling material has a high solar reflectivity in the solar spectral range (0.3–2.5 μm) and a high emissivity in the transparent atmospheric window to achieve sufficient net cooling power.[14–17] So far, passive daytime radiative cooling materials with several different structures have been demonstrated,[18] including photonic structured metamaterials,[19–22] bio-inspired micro-nano structures,[23–26] and 3D fiber network structures.[27,28] At the same time, our research group has also done a lot of research on radiative cooling materials with thin film and coating structures.[29–31]

However, most radiative cooling materials with high reflectivity are white. For windows of vehicles and buildings or objects that need to retain their original colors or high transmittance, such as solar panels, cooling is needed.[32–35] In order to improve the practicality of radiative cooling materials, more and more researchers begin to pay attention to the study of

[a]College of Materials and Chemical Engineering, Hubei Provincial Engineering Research Center for Solar Energy High-value Utilization and Green Conversion, China Three Gorges University, Hubei Provincial, Yichang, China. E-mail: 202208050021009@ctgu.edu.cn

[b]College of Electrical Engineering & New Energy, Hubei Provincial Collaborative Innovation Center for New Energy Microgrid, China Three Gorges University, 8 University Avenue, Yichang, 443002, PR China

[c]State Grid Hubei Direct Current Operation Research Institute, Yichang, Hubei, 443000, China

[d]Department of Mechanical Engineering, University of Western Macedonia, Kozani, 50100, Greece

[e]School of Engineering, University of Leicester, Leicester, LE1 7RH, UK

† Electronic supplementary information (ESI) available: Fig. S1–S10. See DOI: https://doi.org/10.1039/d4ra06819j

transparent radiative-cooling materials. It is still a challenge for transparent radiative-cooling materials to achieve high emissivity (4–25 μm) in the mid-infrared band while maintaining high transmittance in the visible band (380–760 nm).[36,37] Wang *et al.*[38] proposed a pyramid periodic PDMS film, which can achieve 2 °C cooling when encapsulating commercial silicon solar cells. However, the film could not be used on a large scale. Lei *et al.*[39] proposed a transparent double-layer film made of PMMA, modified silica nanoparticles, and Ag, which can achieve a cooling effect of 6 °C below ambient temperature during peak sunlight hours. But the transmittance of the final product made by adding SiO_2 in the method of producing transparent radiative cooling materials is not high.[40] Tu *et al.*[41] proposed a spectrally-selective coating based on tricyclodecane dimethanol diacrylate (DCPDA) monomer, which showed a transmittance of about 90% at visible wavelengths from 400 nm to 800 nm and a thermal emissivity of more than 95% at atmospheric windows (8–13 μm). But in practical applications, radiation refrigeration materials are mostly used outdoors, and long-term exposure to the surface will accumulate dust and dirt, reducing its reflectivity and infrared emissivity, resulting in reduced cooling performance. Especially for transparent radiation refrigeration materials, it will lead to a reduction in its transmittance, further affecting the cooling performance. Therefore, it is necessary to have self-cleaning properties while maintaining its cooling performance and transmittance,[42–46] in order to reduce the need for chemical detergents and the high labor cost of cleaning, reducing the impact on radiative cooling performance,[47,48] reducing the impact on radiative cooling performance. Chen *et al.*[49] demonstrated a transparent ultra-hydrophobic radiative cooling film with an emissivity greater than 85% and a transmittance greater than 90%, which has excellent self-cleaning performance. However, the weather resistance of the film was not discussed. Hu *et al.*[50] obtained STRC composite film by simply treating the cured film of tricyclodecane dimethanol diacrylate (DCPDA). The visible light transmittance of the composite film exceeded 80%, and the mid-infrared emissivity exceeded 95%, showing good self-cleaning performance. But its transmittance is not high. Huang *et al.*[51] proposed a polymer-based microshimon multifunctional metamaterial with a visible light transmittance of 95% and a mid-infrared emissivity of 98%. In the humid Karlsruhe, this metamaterial is about 6 °C lower than the ambient temperature and has good self-cleaning properties. But the production process of this material is more complicated. So far, more and more researchers have begun to pay attention to the research on transparent, self-cleaning and radiative-cooling materials, but most radiative-cooling materials do not have self-cleaning properties, or materials with self-cleaning properties have low visible light transmittance, or have all three properties but the production process is more complex, and the research on related materials is mostly based on coatings. There are not many flexible films available for special-shaped surfaces. In most cases, however, flexible films that can be used on special-shaped surfaces have higher application values.

In this paper, we introduce a method of preparing transparent, self-cleaning and radiative-cooling PVDF composite flexible membrane by solvent evaporation phase conversion.[52] PVDF and PMMA were mixed and dissolved in a certain proportion. After hydrophobic treatment, PPF film was prepared by scraping coating method. The results show that the prepared PPF film has strong mechanical properties, ultraviolet aging resistance, acid and alkali resistance and high flexibility. This discovery is of great significance for the research and development of transparent self-cleaning flexible refrigeration materials.

2. Experimental approach

2.1. Materials used

Poly(vinylidene fluoride) (PVDF) with a molecular weight of 4 000 000 was purchased from MACKLIN, China. Poly(methyl methacrylate) (PMMA) with a specification of heat-resistant optics was purchased from MACKLIN, China. *N*–*N*-Dimethylacetamide (DMAC) with a purity of 99% was purchased from MACKLIN, China. Trimethoxy(1*H*,1*H*,2*H*,2*H*-heptadecafluorodecyl)silane (TMEHFDS) with a purity of 98% was purchased from ALADDIN, China.

2.2. Preparation of transparent hydrophobic aqueous solution

The PVDF and PMMA mixture (7.11 wt%, based on the weight of solvent) was added to the DMAC, stirred at 60 °C until the PVDF and PMMA were completely dissolved. Trimethoxy(1*H*,1*H*,2*H*,2*H*-heptadecafluorodecyl)silane was added to it at different proportion. Trimethoxy(1*H*,1*H*,2*H*,2*H*-heptadecafluorodecyl)silane was stirred in DMAC for 30 minutes at room temperature. The solution was then kept at room temperature for 3 hours.

2.3. Fabrication of transparent hydrophobic film

Using an eyedropper, the solution was carefully dispersed onto the cleaned glass surface, a smooth coating was uniformly formed with an adjustable scraper, and then put in the 100 °C curing oven to obtain the required sample.

2.4. Characterization

2.4.1. Morphological and structural characterization. The surface morphology was observed by field emission scanning electron microscopy (FESEM, JSM-7500F). The chemical properties were analyzed by Fourier near infrared spectroscopy (FTIR, Frontier NIR, PE, USA).

2.4.2. Optical properties. Using a UV-visible spectrophotometer (UV-2550, SHIMADZU), the transmittance of the film in the visible light range (300–900 nm) was determined. A Fourier transform infrared spectrometer (FT-IR, PerkinElmer) was used to measure the emittance of the sample in the mid-infrared region (2–25 μm) and the transmittance at 0.3–2.5 μm.

2.4.3. Wetting states characterization. The contact angle of the sample was measured using the Sci 3000F Contact Angle/Interface System (Beijing Zhongchen Digital Technology Instrument Co., Ltd) in accordance with the established surface characterization scheme. The contact angle of each sample was

determined by measuring a 5 μl water drop, conducting three measurements for each sample, and calculating the average of the three measurements.

2.4.4. Durability test. The durability of the PPF film was assessed through finger friction, tape stripping, and acid and alkali resistance tests. An artificial light source (365 nm, 20 W) was utilized to irradiate the PPF film for investigating its ultraviolet resistance. Following irradiation, the water contact angle (WCA), light transmittance, and radiative cooling performance of the PPF film were quantitatively evaluated.

2.4.5. Cooling performance test. A custom-designed experimental apparatus was developed to evaluate the radiative cooling performance of the PPF film. As illustrated in Fig. 4 a 5 × 5 × 5 cm chamber was dug out of the top of a 15 × 15 × 15 cm rectangular polyethylene foam, and the exposed surface of the device was completely coated with aluminum foil to optimize ambient thermal reflection. During the test, the sample was placed at a height of 5 cm from the bottom of the cavity, and the thermocouple was placed in the middle of the cavity to accurately monitor the temperature of the cavity. To mitigate external convective heat transfer effects on the sample's radiative cooling performance, a layer of transparent polyethylene film was applied to coat the upper surface of the sample. Meteorological parameters such as wind speed and humidity in outdoor environment were measured using a portable handheld meteorological instrument (Shandong Yuntang Intelligent Technology Co., Ltd, Model: YT-SQ05). Solar irradiance levels were quantified using a solar power meter (TES-132). Temperature measurements were conducted utilizing a multi-channel temperature tester (Changzhou Amber Precision Instrument Co., Ltd, Model: AT4208) to assess sample temperatures and quantify its radiative cooling capacity. This device has also been widely used and proved reliable by a large number of researchers studying radiation refrigeration. For example, Qi,[29] Lei,[39] Zhai,[53] *et al.*, also used this device for the radiative cooling tests.

3. Results and discussion

3.1. Analysis of optical properties, hydrophobicity and surface morphology of PPF films

The preparation process of PPF film is shown in Fig. 1. PPF film is prepared by PVDF, PMMA and TMEHFDS. PVDF has excellent anti-aging behavior, climate resistance, UV radiation resistance and other properties, as well as great potential in radiative cooling.[54,55] However, since PVDF is easy to crystallize, its transmittance is not high, and the visible light transmittance (380–760 nm) of pure PVDF film is only 61.5%, as shown in Fig. S1.† From the perspective of microstructure, there is a stick-like structure on the surface of the film, as shown in Fig. 2a. PMMA has the advantages of high transparency and low price, and can effectively inhibit the crystallization of PVDF. The transmittance diagram of PVDF/PMMA film (PP film for short) of different proportions is shown in Fig. S1.† The larger the proportion of PMMA added, the larger the transmittance will be; however, excessive addition of thermoplastic materials will lead to a small number of protrusions or wavy textures on the surface of the film (Fig. S2†). Therefore, the ratio of 8 : 2 was selected to prepare PP film, and the visible light transmittance reached 86%. TMEHFDS was selected for hydrophobic modification of PP films because it has significantly low surface tension. A certain amount of TMEHFDS was added to the PP solution and stirred. When the doping amount of TMEHFDS is 0.22 wt%, the PPF film has good hydrophobicity, the water contact angle can reach 105° or above, and has very high transparency, and the transmittance in the visible light range (380–760 nm) can reach 90% or above (Fig. S3 and S4†). At the same time, we studied the coating thickness. With the increase of coating thickness, the transmittance of PPF film decreased and the hydrophobic angle changed little. When the coating thickness is 0.5 mm, the transmittance of PPF film is the highest, and the transmittance in the visible light range is 94% or above (Fig. S5 and S6†). In addition, the effect of drying

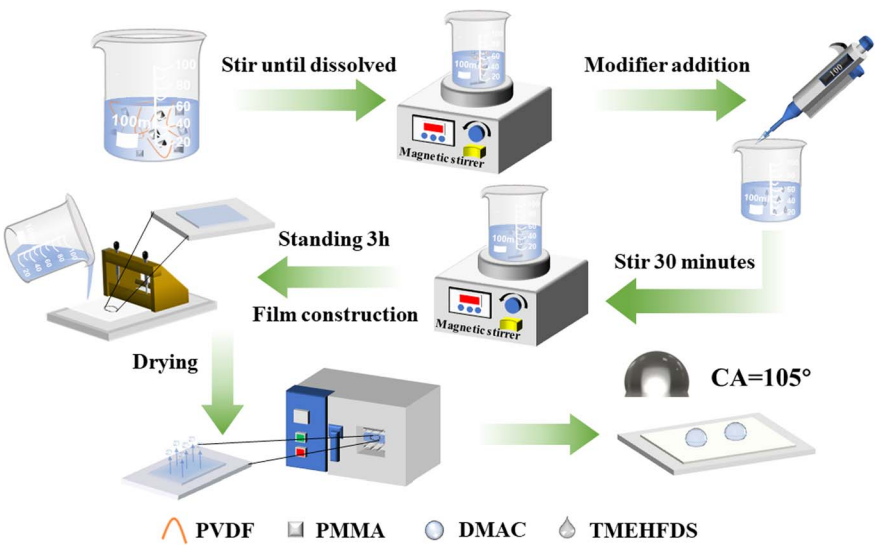

Fig. 1 PPF film preparation flow chart.

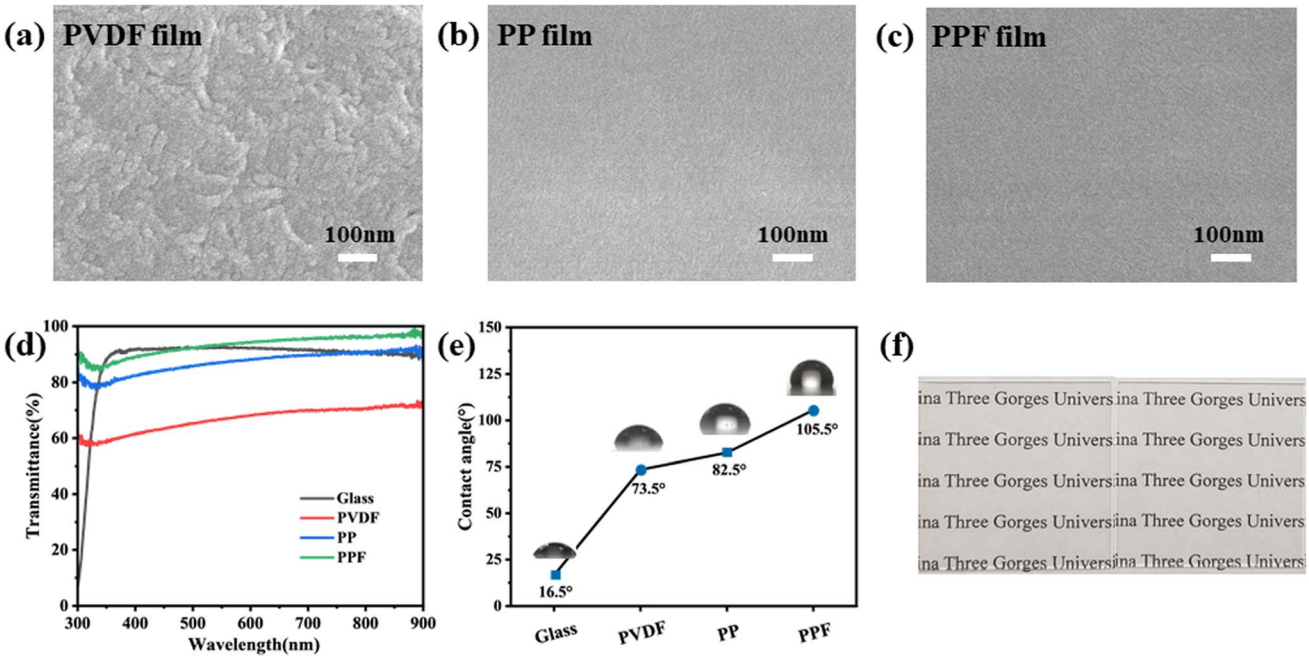

Fig. 2 (a) SEM images of PVDF film; (b) SEM images of PP film; (c) SEM images of PPF film; (d) transmission spectra of bare glass and different modified films; (e) water contact angle between bare glass and different modified films; (f) optical photograph of bare glass (left) and coated with PPF film (right).

temperature on the transmittance of PPF films was investigated. It was found through experiments that when the drying temperature was 100 °C, the transmittance and hydrophobic angle of the prepared PPF film were the largest, as shown in Fig. S7 and S8.† When the drying temperature is low, the solvent evaporates slowly, allowing PVDF more time to rearrange its polymer chain into the lowest energy state. This may result in local crystallization, so its transmittance is not high. While when the drying temperature is high, the rapid evaporation of the solvent is easy to produce an uneven pressure distribution on the film surface, resulting in an uneven structure on the film surface. The drying temperature of 100 °C does not affect the surface morphology of the PPF film, preventing the adjustment of the PVDF polymer chain into a more thermodynamically stable state. Consequently, the polymer chain of PVDF remains disordered, which inhibits the crystallization of PVDF to a certain degree, thereby enhancing the transmittance rate. The rapid evaporation of solvent and the slow crystallization rate lead to the uneven morphology of the membrane surface, which affects the water contact angle of PPF film. Higher drying temperature will further increase the roughness of the film surface resulting in non-uniform structure, which in theory will increase the water contact angle, while lower drying temperature will make the film surface tend to be flat and uniform, usually resulting in a smaller water contact angle. In some cases, the difference in solvent volatilization rate will lead to convection within the solution, affecting the distribution of solutes. Thus affecting the surface properties of the material.

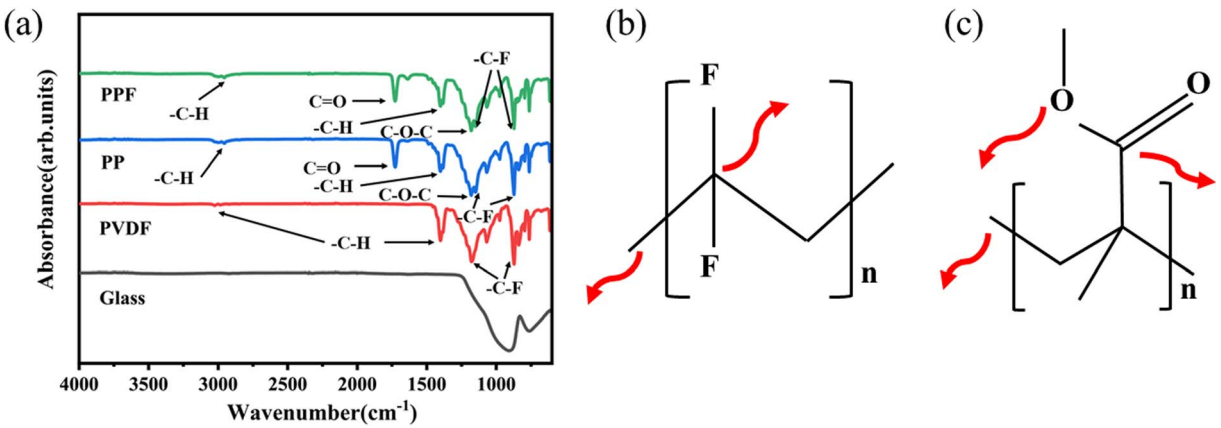

Fig. 3 (a) FTIR spectra of PVDF, PP and PPF films; (b) PVDF molecular formula; (c) PMMA molecular formula.

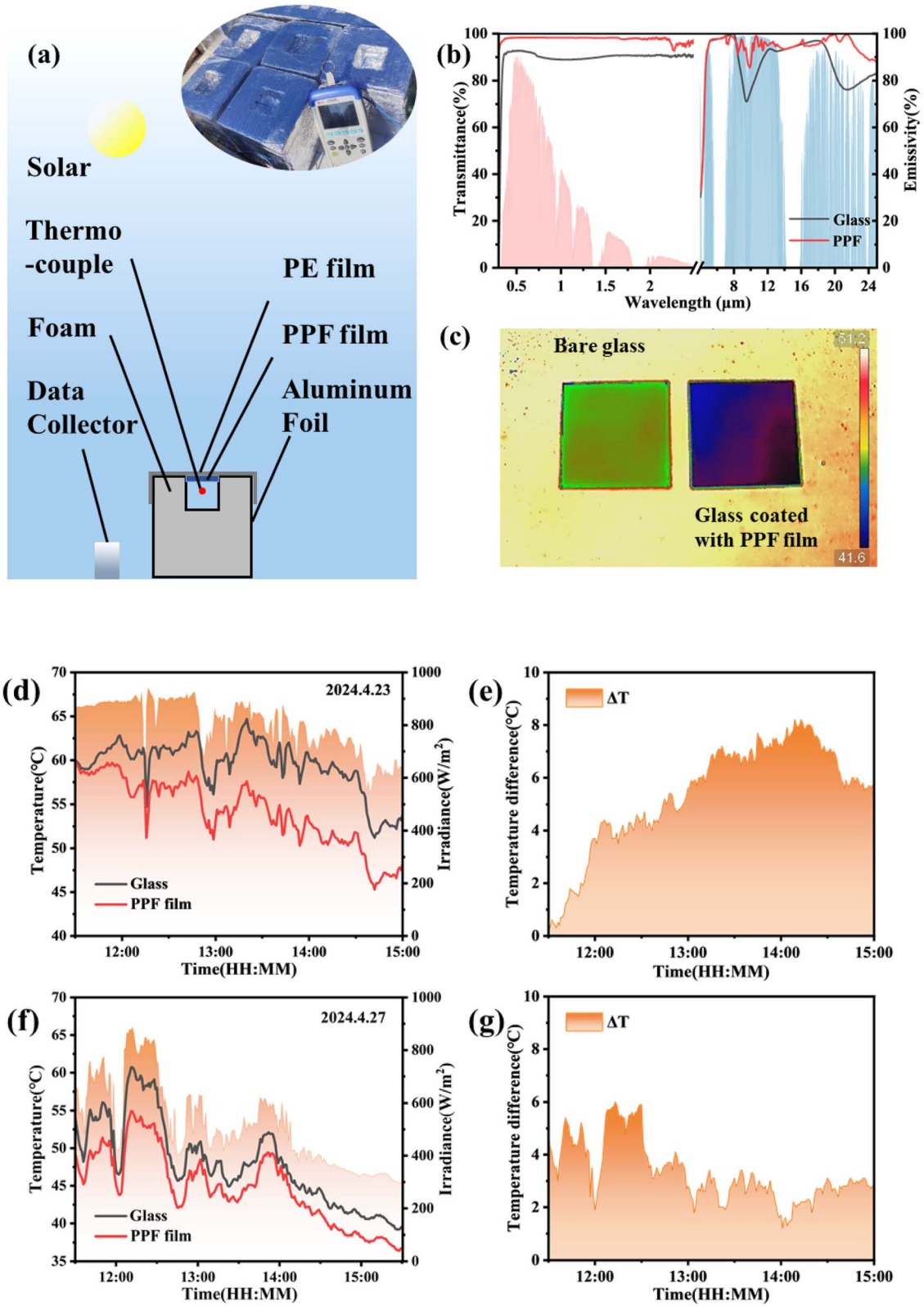

Fig. 4 (a) Schematic and physical drawings of self-made devices; (b) transmittance spectra of 0.3–2.5 μm and emissivity spectra of 4–25 μm for bare glass and PPF coated PPF coated glass; (c) infrared images of bare glass and glass coated with PPF film; (d) daytime temperature variations in the cavities of bare glass and PPF coated glass installations under sunny weather; (e) temperature difference in the cavities of a device coated with PPF film glass and bare glass on sunny weather; (f) daytime temperature variations in the cavities of bare glass and PPF coated glass installations under cloudy weather. (g) Temperature difference in the cavities of a device coated with PPF film glass and bare glass on cloudy weather.

We tested the water contact angle of films formed at different drying temperatures, and found that the water contact angle of films formed at 90 °C was lower, while the difference between the water contact angle of films formed at 100 °C and 110 °C was less than 2°. While considering the transmittance, the drying temperature of 100 °C was selected for the experiment.[56–58] Fig. 2b and c showed the SEM images of PP film and PPF film, respectively. The addition of PMMA inhibited the crystallization of PVDF, so the surfaces of PP film and PPF film were very flat, dense and smooth. The UV-visible transmittance diagram of PVDF, PP and PPF films and the comparison diagram of water contact angle are shown in Fig. 2d and e. Fig. 2f shows the optical photos of bare glass and glass coated with PPF film. As can be seen, the following university names are clearly visible. At the same time, infrared spectrum analysis was performed on PVDF, PP and PPF films, as shown in Fig. 3a. PVDF, PP and PPF films have the stretching vibration of C–H bond at 3300–2800 cm^{-1}. PP and PPF films have the stretching vibration of C=O bond at 2000–1500 cm^{-1}, and the bending vibration of C–H bond, the stretching vibration of C–O–C and C–F bond at 1500–600 cm^{-1}. PVDF film have the bending vibration of C–H bond and the stretching vibration of C–F bond at 1500–600 cm^{-1}. Fig. 3b and c shows the molecular formula of PVDF and PMMA, in which C–H, C–F, C=O and C–O–C groups confirm the results of infrared spectrum analysis. These functional groups of C–H, C–O–C, and C–F bonds have strong absorption or emission in the crowded region (1500–600 cm^{-1}), completely covering the atmospheric window, that is, infrared thermal radiation is transmitted by the atmosphere and the absorption is negligible. According to the above description, PPF film is selected as a good candidate material for radiative cooling.

3.2. Radiative cooling performance test of PPF film

In order to evaluate the radiative cooling performance of PPF film, the real-time temperature of the hollow cavity of the device containing different samples was measured outdoors in Yichang, Hubei Province. The self-made device is placed on the roof of the building, as shown in Fig. 4a, which is a schematic and physical drawing of the self-made device. Fig. 4b shows the transmittance of bare glass and glass-based PPF film at 0.3–2.5 μm and the emissivity of bare glass and glass-based PPF film at 4–25 μm. It can be seen that the near infrared transmittance of PPF film is greater than that of glass. High near infrared transmittance means that the material can transmit radiation more effectively in the near infrared band, reduce the heat accumulation on the surface, and achieve better radiative cooling.[59,60] The emissivity of PPF film is higher than that of glass, and the average emissivity of PPF film reaches 94.42% in the range of 8–13 μm. Fig. 4c shows the infrared images of bare glass and glass coated with PPF film. It can be seen that the surface temperature of glass coated with PPF film is significantly lower than that of bare glass. The PPF film coated on the glass does not cause any occlusion and details about the device can be found in section 2.4.5, where blue represents the sample. The cavity temperature was measured in sunny and cloudy weather respectively, and the experimental temperature data were shown in Fig. 4d–g. Compared with uncoated bare glass, on sunny days, the maximum temperature drop of the cavity coated with PPF film reached 8.2 °C, and the average temperature drop reached 5.4 °C; on cloudy days, the maximum temperature drop of the cavity coated with PPF film reached 6 °C, and the average temperature drop reached 3.3 °C. The reason for certain changes in radiative cooling effect is that when the outdoor temperature, wind speed and humidity change slightly, the relationship between the irradiance, temperature and radiative cooling effect of the sample will also change accordingly. This is because in sunny weather, the attenuation of the radiation transmitted by the atmosphere to the object is small. The atmospheric transmittance is greatly affected by the increase of humidity and cloud cover, which enhances the incident solar radiation and limits the thermal radiation emitted to outer space, resulting in differences in radiative cooling performance within a certain range. This phenomenon can be observed in the temperature data. Data of wind speed and humidity are shown in Fig. S9.† Overall, compared with bare glass, the glass coated with PPF film shows a significant

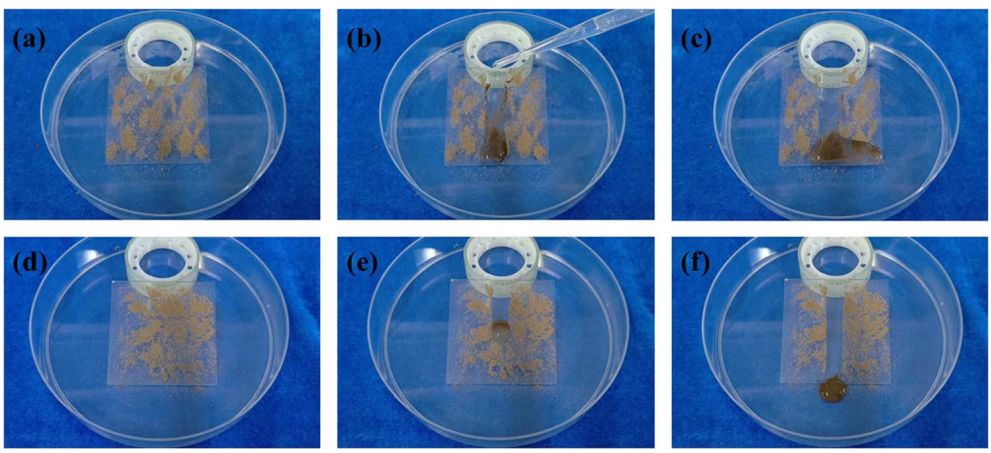

Fig. 5 (a–c) Self-cleaning photo of glass; (d–f) self-cleaning photo of PPF film.

temperature reduction effect on the cavity, which proves that the prepared PPF film has a significant radiative cooling effect.

3.3. Analysis of self-cleaning and durability performance of PPF film

As a material that needs to be used outdoors, its surface is inevitably affected by rain washing, sun exposure and dust deposition, which may affect its optical properties and weaken its radiative cooling performance, which requires PPF films to have self-cleaning properties. In order for us to verify the self-cleaning performance of PPF film, we conducted a self-cleaning performance test. As shown in Fig. 5a–f, the glass is placed at an angle to evenly disperse the sand (simulated pollutants) on the surface of the PPF film and the surface of the bare glass. When water drops on the surface of the bare glass, the water droplets easily penetrate into the pollutants, and the pollutants mixed with water remain on the surface of the glass. On the contrary, when water drops fall on the surface of PPF

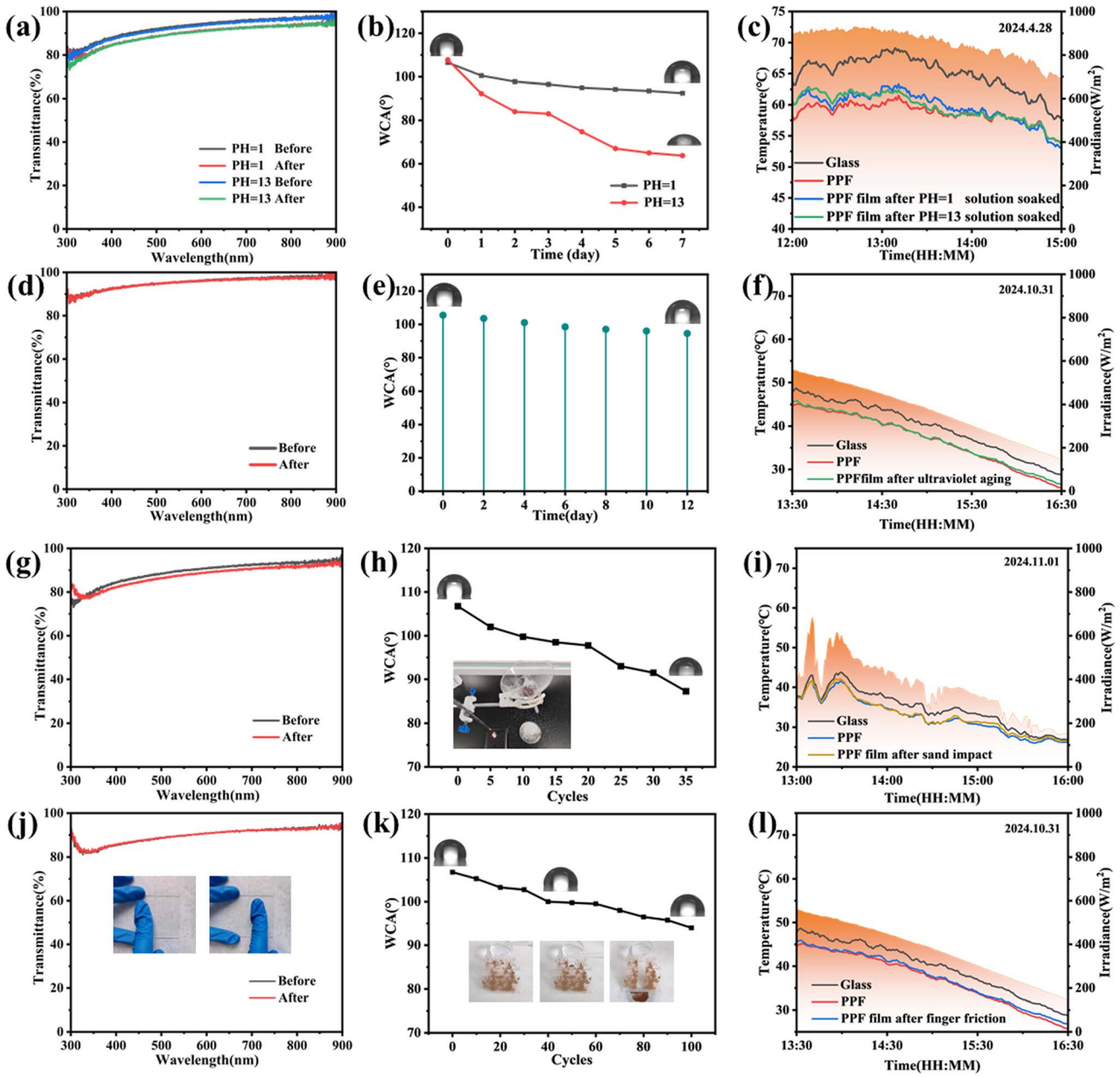

Fig. 6 (a) Transmittance map of PPF film before and after acid and alkali resistance test; (b) change of water contact angle of PPF film with time in solutions with different PH values; (c) comparison of radiative cooling performance of PPF films before and after acid and alkali resistance test; (d) transmittance map of PPF film before and after UV weathering test; (e) change of water contact angle of PPF film with ultraviolet irradiation time; (f) comparison of radiative cooling properties of PPF films before and after UV aging test; (g) transmittance of PPF film before and after sand impact test; (h) change of the water contact angle of PPF film with the number of sand impact; (i) comparison of radiative cooling properties of PPF film before and after sand impact test; (j) transmittance of PPF film before and after finger friction test; (k) change of water contact angle of PPF film with the number of finger friction; (l) comparison of radiative cooling performance of PPF film before and after finger friction test.

film, the water drops will slip off with pollutants, so that the pollutants on the film surface can be easily removed by water. Also, the area washed by water remains transparent, which indicates that PPF film has good self-cleaning performance.

In order for us to verify the durability of PPF film under extreme outdoor conditions, we first tested its acid–alkali resistance. The samples were immersed in solutions with different PH values, and the water contact angles of PPF films with different soaking days were tested and plotted as a chart, as shown in Fig. 6a–c. After soaking in a solution with a pH of 1 for 24 hours, the water contact angle of the sample decreased to 100.5°, after soaking for 48 hours, the water contact angle decreased to 97.75°, and after soaking for one week, the water contact angle decreased to 92.5°. This indicates that although PPF films are affected by strong acids, they still remain hydrophobic.

After soaking in a solution with a pH of 13 for 24 hours, the water contact angle decreased to 92°, after soaking for 48 hours, the water contact angle decreased to 84°, and after soaking for a week, the water contact angle decreased to 63.75°, which can be attributed to the partial hydrolysis of the low surface energy modifying group under strong alkali conditions. PPF film has certain strong acid resistance. The transmittance and radiative cooling properties of PPF films before and after acid and alkali resistance tests were further studied. After the acid and alkali resistance test, the transmittance of PPF film decreased by 3%. After soaking in strong acid, the cooling performance decreased by 1 °C, and after soaking in strong alkali, the cooling performance decreased by 0.9 °C. It is proved that strong acid and base have effect on PPF film's cooling performance, but the effect is not great.

In view of using the scenario of radiative-cooling materials, that is, materials which are exposed to ultraviolet conditions for a long time, it is necessary to carry out ultraviolet aging tests on them. The irradiation intensity was 0.89 W m^{-2} and the temperature was 45 °C, and UV aging test was carried out for PPF films. Fig. 6d shows the change of sample transmittance with the increase of ultraviolet irradiation time. It can be seen that the transmittance of PPF film basically did not change after 12 days of ultraviolet irradiation. Fig. 6f shows the change of water contact angle of the sample with the increase of ultraviolet irradiation time. The hydrophobic angle of the sample decreases with the increase of ultraviolet irradiation time, and the water contact angle drops to 94.5° after 12 days of ultraviolet irradiation. Fig. 6e shows the change of radiative cooling performance of the sample before and after ultraviolet irradiation. In the weather of low irradiance, the cavity of PPF film based on bare glass has a maximum temperature drop of 3.7 °C compared with the cavity of bare glass, and the cooling performance of the sample after ultraviolet aging treatment has basically no change. Therefore, PPF film has certain resistance to ultraviolet aging.

At the same time, the mechanical stability of the PPF film was also evaluated. The mechanical stability of PPF film was verified by sand impact test using sand as friction material. As shown in Fig. 6g–i, the sample was placed in the glass tray at an inclination angle of 30°, a triangular funnel was placed 40 cm above it, the sand weight was set to 20 g, and the contact angle changes were recorded for every 5 impacts. According to results on the surface, after 30 times of sand impact, PPF film still remained in the hydrophobic range, and its transmittance decreased by 2%. Radiative cooling test showed that the radiative cooling test shows that the cooling performance of PPF film has not changed basically. The finger friction experiment was carried out with the finger as the friction object. As shown in Fig. 6j–l, after 100 times of finger friction, the transmittance of PPF film did not change significantly, the water contact angle remained in a hydrophobic state, compared with the PPF film before friction, the radiative cooling performance is basically unchanged. The self-cleaning performance of PPF film after friction was tested, and the self-cleaning performance of PPF

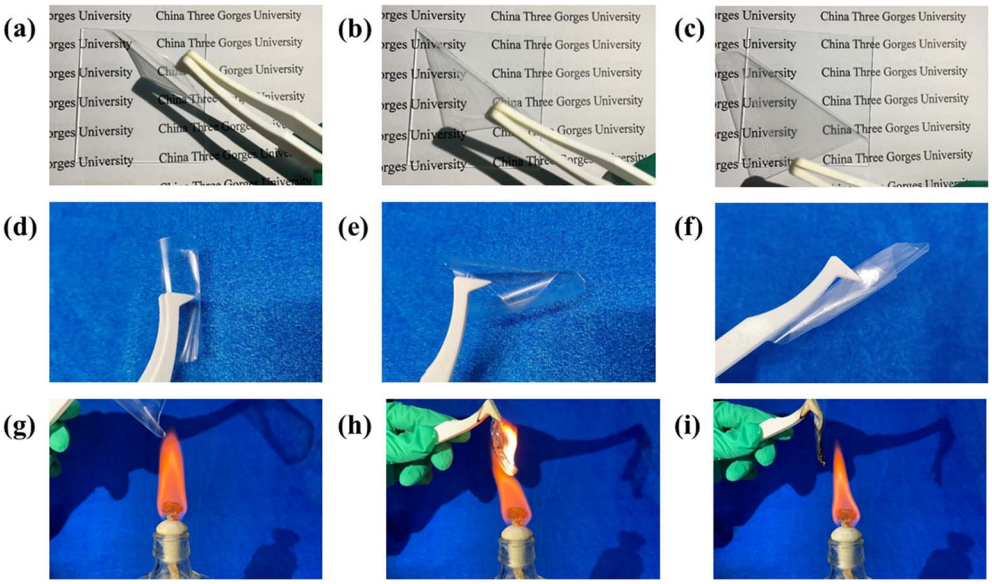

Fig. 7 (a–f) Display of PPF film's flexibility; (g–i) flame retardancy of PPF film.

film after friction was still maintained. This shows that PPF film has a certain mechanical stability.

In addition, liquids of different properties, such as methyl blue, tea, methyl orange, milk and water droplets, were placed on the PPF film to verify the water contact angle. It was found that there were five nearly spherical droplets and the text of the university below the PPF film was clearly visible (Fig. S10†).

3.4. PPF film flexibility, flame retardant performance test

In order to verify the flexible characteristics of the PPF film, as shown in Fig. 7a–f, it can be seen that the PPF film can be torn off the glass substrate at will, and can be crimped to different degrees. Hand twisting and stretching also prove the high flexibility of the film. The excellent flexibility enables PPF films to adapt to different degrees of deformation to meet different shapes of the surface, with a wider range of applications.

When PPF film is used in vehicles or other usage scenarios, its flame retardant performance can make it have a wider application range and higher economic effect. As shown in Fig. 7g–i, the flame retardant performance of PPF film was tested. When the PPF film was ignited, the flame was extinguished quickly and no combustibles fell, indicating PPF film's flame retardant performance.

4. Conclusions

In summary, in this work, we proposed a flexible PVDF composite membrane with transparent, self-cleaning and radiative cooling properties. The resulting PPF film has a transmittance of 94% and above in the visible light range (380–760 nm), and a water contact angle of 105° and above. The PPF film also has self-cleaning performance. The average emissivity in the range of 8–13 μm is 94.42%. As a cooling material, the film has an average sub-ambient temperature drop of 5–6 °C in confined air. At the same time, it has certain mechanical properties, ultraviolet aging resistance and strong acid resistance. In addition, the high flexibility makes the PPF film have a brighter application range and usage value. This work combines the four aspects of transparency, hydrophobicity, radiative cooling and flexibility, and provides a guideline for promoting transparent self-cleaning and radiative cooling films.

Data availability

The data that support the findings of this study are available on request from the corresponding author. The data are not publicly available due to privacy orethical restrictions.

Author contributions

Junxia Mao: conceptualization, data curation, formal analysis, investigation, methodology, supervision, validation, visualization, writing – original draft. Xinyu Tan: conceptualization, data curation, formal analysis, funding acquisition, resources, supervision, writing – review & editing. Weiwei Hu: software. Alkiviadis Tsamis: writing – review & editing. Chao Shi: methodology. Fan Zhou: resources.

Conflicts of interest

The authors declare that they have no known competing financial interests or personal relationships that could have appeared to influence the work reported in this paper.

Acknowledgements

This work was supported by National Natural Science Foundation of China (Grant No. 52007104), Natural Science Foundation of Hubei Province (Grant No. 2022CFD036) and 111 Project (D20015) of China.

References

1 B. Zhao, M. Hu, Q. Xuan, T. H. Kwan, Y. N. Dabwan and G. Pei, Tunable thermal management based on solar heating and radiative cooling, *Sol. Energy Mater. Sol. Cells*, 2022, **235**, 111457, DOI: **10.1016/j.solmat.2021.111457**.

2 M. M. Hossain and M. Gu, Radiative Cooling: Principles, Progress, and Potentials, *Adv. Sci.*, 2016, **3**, 1500360, DOI: **10.1002/advs.201500360**.

3 B. Zhao, M. Hu, X. Ao, N. Chen and G. Pei, Radiative cooling: a review of fundamentals, materials, applications, and prospects, *Appl. Energy*, 2019, **236**, 489–513, DOI: **10.1016/j.apenergy.2018.12.018**.

4 D. Zhao, A. Aili, Y. Zhai, S. Xu, G. Tan, X. Yin and R. Yang, Radiative sky cooling: Fundamental principles, materials, and applications, *Appl. Phys. Rev.*, 2019, **6**, 021306, DOI: **10.1063/1.5087281**.

5 X. Yin, R. Yang, G. Tan and S. Fan, Terrestrial radiative cooling: using the cold universe as a renewable and sustainable energy source, *Science*, 2020, **370**, 786–791, DOI: **10.1126/science.abb0971**.

6 X. Sun, Y. Sun, Z. Zhou, M. A. Alam and P. Bermel, Radiative sky cooling: fundamental physics, materials, structures, and applications, *Nanophotonics*, 2017, **6**, 997–1015, DOI: **10.1515/nanoph-2017-0020**.

7 A. Kamaruddin, T. Wilujeng and M. S. Mahendra, Radiative Cooling for Storage of Vegetables in the Tropics, in *World Renewable Energy Congress VI*, ed. A. A. M. Sayigh, Pergamon: Oxford, 2000, pp. 702–705, DOI: **10.1016/B978-008043865-8/50142-2**.

8 L. Zhou, X. Yin and Q. Gan, Best practices for radiative cooling, *Nat. Sustain.*, 2023, **6**, 1030–1032, DOI: **10.1038/s41893-023-01170-0**.

9 Y. Wang, S. Gao, H. Zhong, B. Zhang, M. Cui, M. Jiang, S. Wang and Z. Wang, Heterogeneous wettability and radiative cooling for efficient deliquescent sorbents-based atmospheric water harvesting, *Cell Rep. Phys. Sci.*, 2022, **3**, 100879, DOI: **10.1016/j.xcrp.2022.100879**.

10 Z. Chen, M. Dong and C. Wang, Passive interfacial photothermal evaporation and sky radiative cooling assisted all-day freshwater harvesting: system design,

experiment study, and performance evaluation, *Appl. Energy*, 2024, **355**, 122254, DOI: 10.1016/j.apenergy.2023.122254.

11 H. D. Wang, C. H. Xue, X. J. Guo, B. Y. Liu, Z. Y. Ji, M. C. Huang and S. T. Jia, Superhydrophobic porous film for daytime radiative cooling, *ACS Appl. Mater. Interfaces*, 2021, **24**, 101100, DOI: 10.1016/j.apmt.2021.101100.

12 X. Li, B. Sun, C. Sui, A. Nandi, H. Fang, Y. Peng, G. Tan and P. Hsu, Integration of daytime radiative cooling and solar heating for year-round energy saving in buildings, *Nat. Commun.*, 2020, **11**, 6101, DOI: 10.1038/s41467-020-19790-x.

13 M. Hossain and M. Gu, Radiative cooling: principles, progress, and potentials, *Adv. Sci.*, 2016, **3**, 1500360, DOI: 10.1002/advs.201500360.

14 Z. Chen, L. Zhu, A. Raman and S. Fan, Radiative cooling to deep sub-freezing temperatures through a 24-h day–night cycle, *Nat. Commun.*, 2016, **7**, 13729, DOI: 10.1038/ncomms13729.

15 N. N. Shi, C. C. Tsai, F. Camino, G. D. Bernard, N. Yu and R. Wehner, Keeping cool: enhanced optical reflection and radiative heat dissipation in saharan silver ants, *Science*, 2015, **349**, 298–301, DOI: 10.1126/science.aab3564.

16 D. Xie, Z. Yang, X. Liu, S. Cui, H. Zhou and T. Fan, Broadband omnidirectional light reflection and radiative heat dissipation in white beetles goliathus goliatus, *Soft Matter*, 2019, **15**, 4294–4300, DOI: 10.1039/C9SM00566H.

17 H. Zhang, K. C. S. Ly, X. Liu, Z. Chen and T. Fan, Biologically inspired flexible photonic films for efficient passive radiative cooling, *Proc. Natl. Acad. Sci. U.S.A.*, 2020, **117**, 14657–14666, DOI: 10.1073/pnas.2001802117.

18 M. M. Huang, M. Yang, X. J. Guo, C. H. Xue, H. D. Wang, *et al.*, Scalable multifunctional radiative cooling materials, *Prog. Mater. Sci.*, 2023, **137**, 0079–6425, DOI: 10.1016/j.pmatsci.2023.101144.

19 E. Rephaeli, A. Raman A and S. Fan, Ultrabroadband photonic structures to achieve high-performance daytime radiative cooling, *Nano Lett.*, 2013, **13**, 1457–1461, DOI: 10.1021/nl4004283.

20 A. P. Raman, M. A. Anoma, L. Zhu, E. Rephaeli and S. Fan, Passive radiative cooling below ambient air temperature under direct sunlight, *Nature*, 2014, **515**, 540–544, DOI: 10.1038/nature13883.

21 S. Y. Jeong, C. Y. Tso, J. Ha, *et al.*, Field investigation of a photonic multi-layered TiO_2 passive radiative cooler in sub-tropical climate, *Renew. Energy*, 2020, **146**, 44–55, DOI: 10.1016/j.renene.2019.06.119.

22 M. M. Hossain, B. Jia and M. Gu, A metamaterial emitter for highly efficient radiative cooling, *Adv. Opt. Mater.*, 2015, **3**, 1047–1051, DOI: 10.1002/adom.201500119.

23 Z. Yan, H. T. Zhai, D. S. Fan and Q. Li, Biological optics, photonics and bioinspired radiative cooling, *Prog. Mater. Sci.*, 2024, **144**, 101291, DOI: 10.1016/j.pmatsci.2024.101291.

24 X. Liu, C. Xiao, P. Wang, *et al.*, Biomimetic photonic multiform composite for high performance radiative cooling, *Adv. Opt. Mater.*, 2021, **9**, 2101151, DOI: 10.1002/adom.202101151.

25 T. Zuo, J. Zhang, S. Zhong, *et al.*, "Cherimoya-like" polysilsequioxane microspheres with structure- enhanced spectral capability for passive daytime radiative cooling, *Mater. Today Commun.*, 2022, **32**, 104096, DOI: 10.1016/j.mtcomm.2022.104096.

26 B. Y. Liu, J. Wu, C. H. Xue, Y. Zeng, J. Liang, S. Zhang, M. Liu, C. Q. Ma, Z. Wang and G. Tao, Bioinspired Superhydrophobic all-in-one coating for adaptive thermoregulation, *Adv. Mater.*, 2024, **36**, 2400745, DOI: 10.1002/adma.202400745.

27 Z. Yan, G. Zhu, D. Fan and Q. Li, Bioinspired Metafabric with Dual-Gradient Janus Design for Personal Radiative and Evaporative Cooling, *Adv. Funct. Mater.*, 2024, 2412261, DOI: 10.1002/adfm.202412261.

28 N. Cheng, D. Miao, C. Wang, Y. Lin, A. A. Babar, X. Wang, Z. Wang, J. Yu and B. Ding, Nanosphere-structured hierarchically porous PVDF-HFP fabric for passive daytime radiative cooling *via* one-step water vapor-induced phase separation, *Chem. Eng. J.*, 2023, **460**, 141581, DOI: 10.1016/j.cej.2023.141581.

29 G. Qi, X. Tan, Y. Tu, X. Yang, Y. Qiao, Y. Wang, J. Geng, S. Yao and X. Chen, Ordered-Porous-Array Polymethyl Methacrylate Films for Radiative Cooling, *ACS Appl. Mater. Interfaces*, 2022, **14**, 31277–31284, DOI: 10.1021/acsami.2c06809.

30 S. Nie, X. Tan, X. Li, K. Wei, T. Xiao, L. Jiang, J. Geng, Y. Liu, W. Hu and X. Chen, Facile and Environmentally-Friendly Fabrication of Robust Composite Film with Superhydrophobicity and Radiative Cooling Property, *Compos. Sci. Technol.*, 2022, **230**, 109750, DOI: 10.1016/j.compscitech.2022.109750.

31 W. Hu, F. Zhang, X. Tan, Y. Tu and S. Nie, Antibacterial PVDF Coral-Like Hierarchical Structure Composite Film Fabrication for Self-Cleaning and Radiative Cooling Effect, *ACS Appl. Mater. Interfaces*, 2024, **16**, 19828–19837, DOI: 10.1021/acsami.4c01926.

32 C. G. Granqvist, A. Hjortsberg and T. S. Eriksson, Radiative cooling to low temperatures with selectivity IR-emitting surfaces, *Thin Solid Films*, 1982, **90**, 187–190, DOI: 10.1016/0040-6090(82)90648-4.

33 A. R. Gentle and G. B. Smith, Radiative Heat Pumping from the Earth Using Surface Phonon Resonant Nanoparticles, *Nano Lett.*, 2010, **10**, 373–379, DOI: 10.1021/nl903271d.

34 S. Catalanotti, V. Cuomo, G. Piro, D. Ruggi, V. Silvestrini and G. Troise, The radiative cooling of selective surfaces, *Sol. Energy*, 1975, **17**, 83–89, DOI: 10.1016/0038-092X(75)90062-6.

35 S. Gamage, E. S. H. Kang, C. Åkerlind, S. Sardar, J. Edberg, H. Kariis, T. Ederth, M. Berggren and M. P. Jonsson, Transparent nanocellulose metamaterial enables controlled optical diffusion and radiative cooling, *J. Mater. Chem. C*, 2020, **8**, 11687–11694, DOI: 10.1039/D0TC01226B.

36 J. Yeonghoon, J. Youngjae and Y. Kyoungsik, Infrared-Reflective Transparent Hyperbolic Metamaterials for Use in Radiative Cooling Windows, *Adv. Funct. Mater.*, 2022, **3**, 2207940, DOI: 10.1002/adfm.202207940.

37 B. Zhao, M. Hu, X. Ao and G. Pei, Performance analysis of enhanced radiative cooling of solar cells based on a commercial silicon photovoltaic module, *Sol. Energy*, 2018, **176**, 248–255, DOI: 10.1016/j.solener.2018.10.043.

38 K. Wang, G. Luo, X. Guo, S. Li, Z. Liu and C. Yang, Radiative cooling of commercial silicon solar cells using a pyramid-textured PDMS film, *Sol. Energy*, 2021, **225**, 245–251, DOI: 10.1016/j.solener.2021.07.025.

39 M. Lei, Y. Hu, Y. Song, Y. Li, Y. Deng, K. Liu, L. Xie, J. Tang, D. Han, J. Lei and Z. Li, Transparent radiative cooling films containing poly(methylmethacrylate), silica, and silver, *Opt. Mater.*, 2021, **122**, 111651, DOI: 10.1016/j.optmat.2021.111651.

40 R. Palkovits, H. Althues, A. Rumplecker, B. Tesche, A. Dreier, U. Holle, G. Fink, C. H. Cheng, D. F. Shantz and S. Kaskel, Polymerization of w/o microemulsions for the preparation of transparent SiO_2/PMMA, Nanocomposites, *Langmuir*, 2005, **21**, 6048–6053, DOI: 10.1021/la050630k.

41 Y. Tu, X. Tan, G. Qi, X. Yang, X. Ouyang, W. Yan, W. Hu, J. Geng and R. Yang, Transparent, anti-corrosion and high broadband emission coating for zero energy consumption cooling technology, *Mater. Today Phys.*, 2023, **34**, 101070, DOI: 10.1016/j.mtphys.2023.101070.

42 A. Eshaghi, M. Mesbahi and A. A. Aghaei, Transparent hierarchical micro-nano structure PTFE-SiO_2 nanocomposite thin film with superhydrophobic, self-cleaning and anti-icing properties, *Optik*, 2021, **241**, 166967, DOI: 10.1016/j.ijleo.2021.166967.

43 Y. L. Zhan, M. Ruan, W. Li, H. Li, L. Y. Hu, F. M. Ma, Z. L. Yu and W. Feng, Fabrication of anisotropic PTFE superhydrophobic surfaces using laser microprocessing and their self-cleaning and anti-icing behavior, *Colloids Surf., A*, 2017, **535**, 8–15, DOI: 10.1016/j.colsurfa.2017.09.018.

44 W. Zeng, J. Chen, H. Yang, L. Deng, G. Liao and Z. Xu, Robust coating with superhydrophobic and self-cleaning properties in either air or oil based on natural zeolite, *Surf. Coat. Technol.*, 2017, **309**, 1045–1051, DOI: 10.1016/j.surfcoat.2016.10.036.

45 K. Ravi, W. L. Sulen, C. Bernard, Y. Ichikawa and K. Ogawa, Fabrication of micro-/nano-structured super-hydrophobic fluorinated polymer coatings by cold-spray, *Surf. Coat. Technol.*, 2019, **373**, 17–24, DOI: 10.1016/j.surfcoat.2019.05.078.

46 M. Liu, X. Tan, X. Li, J. Geng, M. Han, K. Wei and X. Chen, Transparent superhydrophobic EVA/SiO_2/PTFE/KH-570 coating with good mechanical robustness, chemical stability, self-cleaning effect and anti-icing property fabricated by facile dipping method, *Colloids Surf., A*, 2023, **658**, 130624, DOI: 10.1016/j.colsurfa.2022.130624.

47 G. B. Darband, M. Aliofkhazraei, S. Khorsand, S. Sokhanvar and A. Kaboli, Science and Engineering of Superhydrophobic Surfaces: Review of Corrosion Resistance, Chemical and Mechanical Stability, *Arabian J. Chem.*, 2020, **13**, 1763–1802, DOI: 10.1016/j.arabjc.2018.01.013.

48 S. Das, S. Kumar, S. K. Samal, S. Mohanty and S. K. Nayak, A Review on Superhydrophobic Polymer Nanocoatings: Recent Development and Applications, *Ind. Eng. Chem. Res.*, 2018, **57**, 2727–2745, DOI: 10.1021/acs.iecr.7b04887.

49 G. Chen, Y. Wang, J. Qiu, J. Cao, Y. Zou, S. Wang, J. Ouyang, D. Jia and Y. Zhou, A visibly transparent radiative cooling film with self-cleaning function produced by solution processing, *J. Mater. Sci. Technol.*, 2021, **90**, 76–84, DOI: 10.1016/j.jmst.2021.01.092.

50 W. Hu, X. Tan, X. Yang, G. Qi, S. Chen, S. Li, Y. Wang, F. Zhang, K. Yan and Z. Kang, A superhydrophobic transparent radiative cooling film exhibits excellent resistance to acid and alkali as well as remarkable robustness, *Opt. Mater.*, 2024, **149**, 114995, DOI: 10.1016/j.optmat.2024.114995.

51 G. Huang, A. R. Yengannagari, K. Matsumori, *et al.*, Radiative cooling and indoor light management enabled by a transparent and self-cleaning polymer-based metamaterial, *Nat. Commun.*, 2024, **15**, 3798, DOI: 10.1038/s41467-024-48150-2.

52 J. Zhou, X. Man, Y. Jiang and M. Doi, Structure Formation in Soft-Matter Solutions Induced by Solvent Evaporation, *Adv. Mater.*, 2017, **29**, 1703769, DOI: 10.1002/adma.201703769.

53 Y. Zhai, Y. Ma, S. N. David, D. Zhao, R. Lou, G. Tan, R. Yang and X. Yin, Scalable-manufactured randomized glass-polymer hybrid metamaterial for daytime radiative cooling, *Science*, 2017, **355**, 1062–1066, DOI: 10.1126/science.aai7899.

54 J. Mandal, Y. Fu, A. C. Overvig, M. Jia, K. Sun, N. N. Shi, H. Zhou, X. Xiao, N. Yu and Y. Yang, Hierarchically porous polymer coatings for highly efficient passive daytime radiative cooling, *Science*, 2018, **362**, 315–319, DOI: 10.1126/science.aat9513.

55 X. Wang, X. Liu, Z. Li, H. Zhang, Z. Yang, H. Zhou and T. Fan, Scalable flexible hybrid membranes with photonic structures for daytime radiative cooling, *Adv. Funct. Mater.*, 2019, **30**, 1907562, DOI: 10.1002/adfm.201907562.

56 J. Cummings, J. S. Lowengrub, B. G. Sumpter, *et al.*, Modeling solvent evaporation during thin film formation in phase separating polymer mixtures, *Soft Matter*, 2018, **14**, 1833–1846, DOI: 10.1039/C7SM02560B.

57 A. Statt, M. P. Howard and A. Panagiotopoulos, Solvent quality influences surface structure of glassy polymer thin films after evaporation, *J. Chem. Phys.*, 2017, **147**, 184901, DOI: 10.1063/1.4996119.

58 S. Khan, K. Wang, G. Yuan, *et al.*, Marangoni Effect during Solvent Evaporation: Its Influence on Film Formation and Surface Properties, *Sci. Rep.*, 2017, **7**, 5292, DOI: 10.1038/s41598-017-05506-7.

59 A. P. Raman, M. A. Abou, L. Zhu, *et al.*, Passive radiative cooling below ambient air temperature under direct sunlight, *Nature*, 2014, **515**, 540–544, DOI: 10.1038/nature13883.

60 L. Zhu, A. P. Raman and S. Fan, Radiative cooling of solar absorbers using a visibly transparent photonic crystal thermal blackbody, *Proc. Natl. Acad. Sci. U. S. A.*, 2015, **112**, 12282–12287, DOI: 10.1073/pnas.1509453112.